

On the similarity and challenges of multiresonant and iterative learning current controllers for grid converters and why the disturbance feedforward matters

Abstract. There are two main techniques to solve the reference tracking problem for repetitive references and under repetitive disturbances, namely multiresonant (a.k.a. multioscillatory) controllers and iterative learning controllers. Nevertheless, neither of the approaches is a definitive winner, which is to be demonstrated herein. Both have their strengths, weaknesses and challenges. A grid-tie converter will be the case study here. The goal is to draw or inject sinusoidal currents under distorted grid voltage conditions. The supporting feedforward controller will be addressed within the context of the discussed repetitive control task. The case will be illustrated using numerical simulations. Our main goal is to make practitioners familiar with the relationships between these two control methods.

Streszczenie. Istnieją dwa główne sposoby rozwiązywania zadania regulacji nadążnej dla powtarzalnego sygnału zadanego w obecności powtarzalnego zakłócenia, jest to zastosowanie regulatorów wielorezonansowych (zwanymi też wielooscylicyjnymi) oraz regulatorów z uczeniem iteracyjnym. Jednak żadnego z tych rozwiązań nie można uznać za jednoznacznie lepsze, co zostanie tutaj pokazane. Oba cechują zarówno mocne strony, jak i pewne słabości oraz wyzwania implementacyjne. Przekształtnik sieciowy posłuży tutaj za przykład. Celem jest pobieranie lub oddawanie sinusoidalnego prądu sieci pomimo odkształconego napięcia. Omówione zostanie również sprzężenie w przód od zakłócenia w kontekście zadania sterowania powtarzalnego. Zagadnienie zostanie zilustrowane przy użyciu symulacji komputerowych. Naszym głównym celem jest pokazanie praktykom związków pomiędzy tymi dwiema metodami sterowania. (O podobieństwach i wyzwaniach regulatorów wielorezonansowych i regulatorów z uczeniem iteracyjnym dla przekształtników sieciowych oraz dłączonego sprzężenia w przód ma znaczenie)

Keywords: repetitive control, iterative learning control, multiresonant controller, grid converter, disturbance feedforward

Słowa kluczowe: sterowanie powtarzalne, sterowanie z uczeniem powtarzalnym, regulator wielorezonansowy, przekształtnik sieciowy, sprzężenie w przód od zakłócenia

Introduction

It is not uncommon that the iterative learning community members are convinced that their controllers are superior in performance to the multiresonant control schemes. Surprisingly, it also seems to prevail that the designers of multiresonant controllers for grid converters and true sine wave inverters are often not aware that there exists a family of iterative learning control (ILC) laws that is exceptionally simple in implementation, and that the very basic ILC controller can offer similar steady-state errors as the multiresonant controller. Our goal is to make both groups of engineers familiar with both techniques.

To begin with, it is necessary to select a common nomenclature. There is no definitive consensus on naming here. Historically, repetitive control was developed for continuous repetitive processes, whereas iterative learning control (ILC) was proposed within the context of batch repetitive processes. After that naming conventions and categorizations only got more and more complicated. The fact is that most ILC techniques can be used successfully for both continuous and batch repetitive processes. Moreover, some authors refer to multiresonant controllers as something that falls outside repetitive control (e.g. [1, 2]), which is rather questionable. We do not feel to be in the position to sort the naming once and for all. However, for the purpose of this paper we propose the following categorization: a repetitive controller is any controller that takes into account (explicitly or implicitly) the repetitiveness of the reference and the disturbance to reduce control errors. Within the repetitive control systems we then distinguish two main techniques: multiresonant control that can be applied only to continuous repetitive processes and iterative learning control that is somewhat more versatile because it can be applied for any type of repetitive control task. We would also like to clarify that 'repetitive' and 'periodic', despite often being used interchangeably to characterize a signal, may be also used more specifically. All periodic signals are repetitive ones, but not all repetitive signals have to be periodic in a mathematical sense. For example, in laser cutting machines the cutting itself is repetitive and should be

managed using a repetitive control technique, but the process of positioning the tool for each cut can be non-repetitive and thus would be governed by a non-repetitive controller. The process itself is then repetitive, although the overall trajectory for the tool does not have to be periodic. For the illustration see Fig. 1. This is typical in batch processes, in which we reset the initial conditions for each repetition. That is why multiresonant control is generally not suitable for batch processes. However, if the initial state of the batch is equal to its final state, as in Fig. 1), it is still possible to implement the multioscillatory controller by setting its initial state equal to its final state from the previous batch.

This paper deals with a continuous repetitive process of energy conversion using a grid-tie converter and no state resetting at the beginning of the pass (=period) is possible. Therefore, the discussion of repetitive control for batch processes is out of the scope and we focus on systems with strictly periodic references and disturbances – systems eligible for multiresonant control as well as ILC. Both techniques stem from the internal model principle as they both insert a model of the periodic signal in the control loop.

This is neither a survey paper, nor does it contain previously unpublished control schemes. Nevertheless, we strongly believe that there is a need for such a potentially eye-opening case study – mainly to bring both parties to the table, and maybe back to the drawing board.

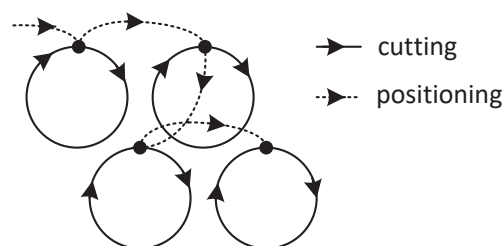


Fig. 1. An example of a repetitive cutting process with a non-periodic overall trajectory for a tool (cutting plus positioning).

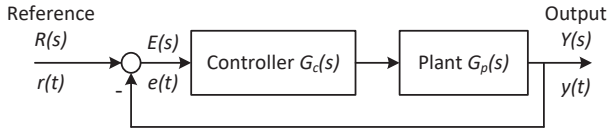


Fig. 2. A closed-loop control system.

Internal model principle

The internal model principle (IMP) is probably one of the most important concepts regarding tracking control systems, yet surprisingly it often remains obscure to many practitioners. For the sake of brevity, we are not going to retell herein the whole theory for SISO and MIMO control systems. For more details please refer e.g. to [3, 4, 5] or handouts [6, 7]. Nevertheless, to make the paper more complete, a simplified analysis for an SISO system is presented, which is mostly based on [6].

Let us consider the feedback control system depicted in Fig. 2 and denote numerators and denominators as follows

$$(1) \quad R(s) = \frac{N_r(s)}{D_r(s)}$$

$$(2) \quad G_c(s) = \frac{N_c(s)}{D_c(s)}$$

$$(3) \quad G_p(s) = \frac{N_p(s)}{D_p(s)},$$

where subscripts \bullet_r , \bullet_c and \bullet_p indicate the reference, the controller and the plant, respectively. The purpose of the controller is twofold. First, it has to provide stability of the closed-loop system. Second, it should regulate the output $y(t)$ in a specified manner to meet the required performance. If the objective is to force control error $e(t)$ to decay asymptotically towards zero

$$(4) \quad \lim_{t \rightarrow \infty} e(t) = \lim_{s \rightarrow 0} sE(s) = 0,$$

the poles of $E(s)$ have to be in the open left half plane, i.e. $\Re(s) < 0$. Writing down the equation for the summation node in Fig. 2, we get

$$(5) \quad E(s) = R(s) - E(s)G_c(s)G_p(s),$$

which in turn gives

$$(6) \quad E(s) = \frac{1}{1 + G_c(s)G_p(s)} R(s).$$

Substituting (1)–(3), we produce the transfer function

$$(7) \quad E(s) = \frac{D_c(s)D_p(s)}{D_c(s)D_p(s) + N_c(s)N_p(s)} \frac{N_r(s)}{D_r(s)}.$$

Now let us assume that the condition (4) has to be met for the reference signal $r(t)$ whose Laplace transform has poles in the closed right half plane, i.e. $\Re(s) \geq 0$. This is the case of periodic signals, for which $\Re(s) = 0$. Obviously, designing the controller only for asymptomatic stability of the closed loop-system, by placing the closed-loop poles of

$$(8) \quad P_{cl}(s) = D_c(s)D_p(s) + N_c(s)N_p(s)$$

in the open left half plane, does not guarantee zero steady state errors under $D_r(s)$ with roots in the closed right half plane. This is because these roots are also the poles of (7). The only possibility to draw control errors towards zero

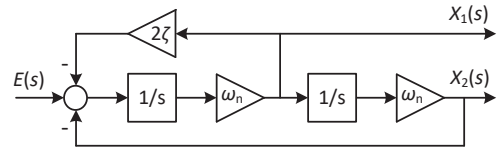


Fig. 3. An oscillatory element.

is then to cancel these poles using roots of $D_c(s)D_p(s)$. If some of these poles are not naturally present in the plant itself ($D_p(s)$), they have to be introduced in the controller ($D_c(s)$). The design workflow is then as follows:

- 1) decide on your reference signal shape, i.e. assume a specific $D_r(s)$, also known as the generating polynomial;
- 2) identify roots of $D_p(s)$;
- 3) if a minimalistic structure of a controller is expected, design its structure to have $D_c(s)$ that introduces all the roots of $D_r(s)$ not present in $D_p(s)$, i.e. build the missing part of the generating polynomial into the controller;
- 4) design gains of the controller appropriately to move all the roots of the closed-loop characteristic polynomial (8) into the open left half plane.

It should be noted that the IMP lets you design the structure of the controller, which is the step prior to the tuning procedure.

Summarizing this section, the internal model principle is indispensable in determining the minimal structure of the controller required to get zero tracking errors for a given reference signal. Under $R(s)$ having the poles in the closed right half plane, $\lim_{t \rightarrow \infty} e(t) = 0$ can be expected if and only if $D_r(s)$ is a factor of the open-loop characteristic polynomial $D_c(s)D_p(s)$, i.e., there exists such an $O(s)$ that $D_c(s)D_p(s) = D_r(s)O(s)$, and obviously all the closed-loop poles are in the open left half plane. The resulting controller provides

$$(9) \quad E(s) = \frac{O(s)N_r(s)}{D_c(s)D_p(s) + N_c(s)N_p(s)},$$

which allows the control error to decay asymptotically towards zero as all the poles of (9) are in the open left half plane. Similar analyses can be done for input and output disturbances [7], and their results lead to a more general formulation of the internal model principle: if an input disturbance or a reference have $D(s)$ as the generating polynomial, the controller that introduces the missing part of the generating polynomial into the open-loop system can asymptotically reject the effect of disturbance and cause the output to track the reference.

It is worth noticing at this point that the IMP can be used explicitly as described above to determine the structure of the controller using a generating polynomial, as well as implicitly to introduce an internal model of the reference or disturbance signals in forms other than generating polynomials. Such implicit models of signals are constructed iteratively in the classic iterative learning controllers [8, 9], as well as in the dynamic optimization based ones [10, 11, 12, 13]. The former ones are to be compared here in computer simulations to the explicit multiresonant ones.

Model of the input using resonant/oscillatory elements

If the grid voltage is symmetrical and not distorted, it is enough to implement PI current controllers in the rotating dq reference frame aligned with the grid voltage space vector to track sinusoidal reference currents. This is because the d - and q -component are constant in the steady state, and integration (I) constitutes the model of a constant signal. How-

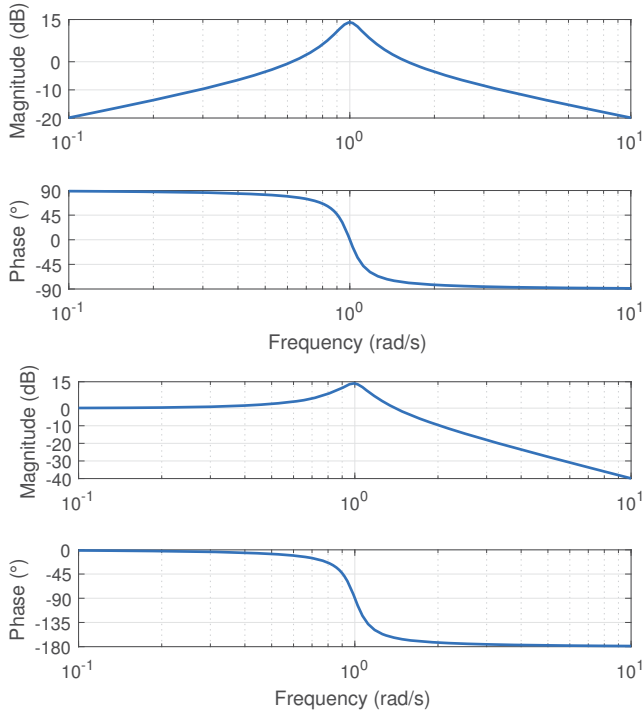


Fig. 4. A comparison of Bode plots for $G_1(s)$ [on the top] and $G_2(s)$, assuming $\omega_n = 1$ and $\zeta = 0.1$.

ever, for a distorted grid voltage containing higher harmonics, being a disturbance to the system, it is no longer possible to track sinusoidal reference current, unless a model of the disturbance is included in the controller. One of the techniques to tackle this is to introduce oscillatory elements to the controller. An oscillatory element shown in Fig. 3 has two state variables

$$(10) \quad G_1(s) = \frac{X_1(s)}{E(s)} = \frac{\omega_n s}{s^2 + 2\zeta\omega_n s + \omega_n^2}$$

and

$$(11) \quad G_2(s) = \frac{X_2(s)}{E(s)} = \frac{\omega_n^2}{s^2 + 2\zeta\omega_n s + \omega_n^2},$$

where ζ is the damping ratio and ω_n is the natural frequency (precisely: angular frequency or pulsance) of a harmonic oscillator. To achieve a theoretically perfect tracking of a given harmonics it is required to set $\zeta = 0$. However, for most applications this is impractical. It should be noted that the amplitudes of both state variables x_1 and x_2 grow into infinity if the pulsance ω_n cannot be totally eliminated from the control error, e.g. due to the limitations on the actuator or plant side. That is why some degree of damping is recommended. This damping does not have to be constant – it is common practice to vary it according to the state of the actuator (in our case the converter), and increase it if the actuator saturates [14].

If the oscillator is used as a part of an augmented full-state feedback controller, both state variables x_1 and x_2 are naturally taken as feedback variables. However, if one of the variables is to be chosen for e.g. a proportional-resonant (PR) controller (not of a full-state type), x_1 should be used. This can be clearly read from Fig. 4: $G_1(s)$ is a bandpass filter, whereas $G_2(s)$ is a second order low-pass filter. Both of them have the same bump at ω_n , but the latter is not selective. This selectiveness of the former filter is highly desired, especially if expert/heuristic tuning methods are to be involved.

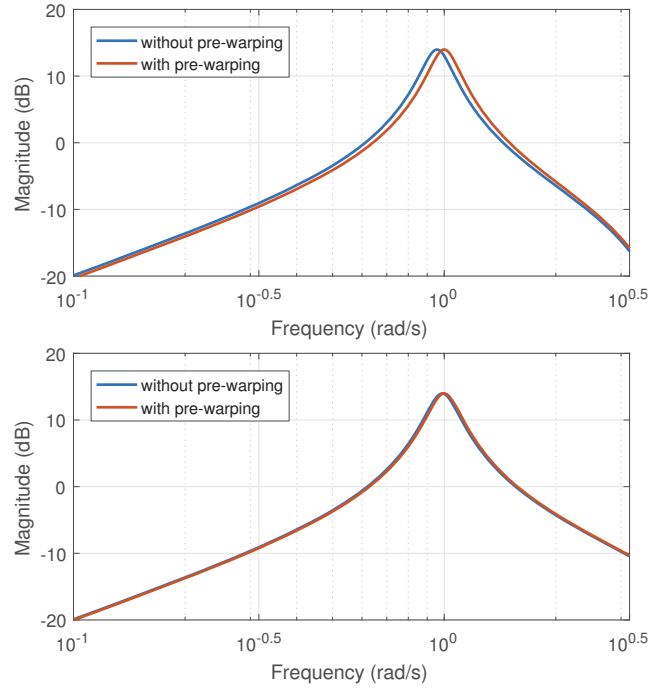


Fig. 5. The influence of pre-warping for $\frac{8.33}{2\pi}$ Hz sampling [on the top] and for the two times faster sampling (the expected resonant frequency at 1 rad/s).

By discretizing $G_1(s)$ using e.g. the bilinear transform (Tustin's method), we shift the resonant frequency. This effect is not significant if the natural frequency of the oscillatory element is far from the sampling frequency. However, it is good practice to always correct for this effect, as this is done offline and does not increase the complexity of the controller itself. The procedure is called pre-warping the filter design. The resonant frequency matching for bilinear transform is achieved by shifting the ω_n for the continuous-time domain transfer function before discretization. The formula is

$$(12) \quad \omega_n = \frac{2}{T_s} \tan\left(\omega_d \frac{T_s}{2}\right),$$

and then we proceed with the regular bilinear transform substituting

$$(13) \quad s \leftarrow \frac{T_s}{2} \frac{1 - z^{-1}}{1 + z^{-1}},$$

where T_s is the sampling time and ω_d is the desired resonant frequency for the discrete oscillator. For more details please see [15, 16]. The effect of pre-warping is illustrated in Fig. 5. Obviously, the mismatch increases along with the increasing resonant frequency of the oscillatory element in respect to the sampling frequency. If the Nyquist frequency and the resonant frequency are more than one decade apart, the improvement is rather negligible for most control systems. However, if they are closer than one decade, pre-warping should be employed to get the most from the oscillatory controller. And as already mentioned, pre-warping costs us nothing in terms of real-time implementation, therefore it is always better to perform it – regardless of the placement of the resonant frequency in respect to the Nyquist frequency.

To facilitate the comparison presented two sections forward, it should be noted that introducing a delay to (10) or (11) does not change their ability to generate a sinusoidal signal. Also, a negative gain does not render the element impractical, as the overall phase is the key point here – not just a sign. For example, negative gains for oscillatory terms

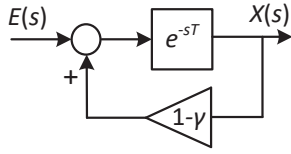


Fig. 6. A universal periodic signal generator.

are common when an LQR is used to tune the controller. The exemplary resulting sinusoidal waveform generators, such as

$$(14) \quad G_3(s) = G_1(s)e^{-s\frac{2\pi}{\omega_n}}$$

or

$$(15) \quad G_4(s) = -G_1(s)e^{-s\frac{\pi}{\omega_n}},$$

could be used as a replacement for $G_1(s)$. Obviously, we do not introduce additional half-cycle or full-cycle delays to the oscillatory term in a regular resonant controller. This would hamper the innate ability of an oscillatory controller to correct the control signal without the necessity to wait an entire pass (=period of the reference signal). However, we will use them as viable alternatives while demonstrating similarities to the ILC.

Model of the input using a universal periodic signal generator

Another approach to creating an internal model of the repetitive signal is to use the universal periodic signal generator shown in Fig. 6. Its transfer function is as follows

$$(16) \quad G_5(s) = \frac{1}{e^{sT} - (1 - \gamma)},$$

where T is the period of the reference signal and γ is the forgetting factor. Note that for $\gamma = 0$ this system simply integrates in the pass to pass direction. Its discrete representation is as follows

$$(17) \quad x(k, p) = (1 - \gamma)x(k - 1, p) + e(k - 1, p),$$

where k is the pass index and p is the sample number along the pass.

Are they equivalent or just similar?

Let us start from the definition of the hyperbolic sinus

$$(18) \quad \sinh\left(\frac{sT}{2}\right) \triangleq \frac{e^{\frac{sT}{2}} - e^{-\frac{sT}{2}}}{2} = \frac{e^{sT} - 1}{2e^{\frac{sT}{2}}}$$

and an infinite product representation of the hyperbolic sinus [17]

$$(19) \quad \sinh\left(\frac{sT}{2}\right) = \frac{sT}{2} \prod_{n=1}^{\infty} \left(1 + \left(\frac{sT}{2\pi n}\right)^2\right).$$

Now, let us assume that we have an integral-multiresonant controller $C_1(s)$ to introduce an internal model of any periodic signal

$$(20) \quad C_1(s) = \frac{k_0}{s} + \sum_{n=1}^{\infty} \frac{k_n s}{\left(\frac{s}{n\omega_1}\right)^2 + 1},$$

where $\omega_1 = \frac{2\pi}{T}$ is the fundamental pulsance. Its generating polynomial is as follows

$$(21) \quad D_1(s) = s \prod_{n=1}^{\infty} \left(\left(\frac{s}{n\omega_1}\right)^2 + 1\right) = s \prod_{n=1}^{\infty} \left(\left(\frac{sT}{2\pi n}\right)^2 + 1\right).$$

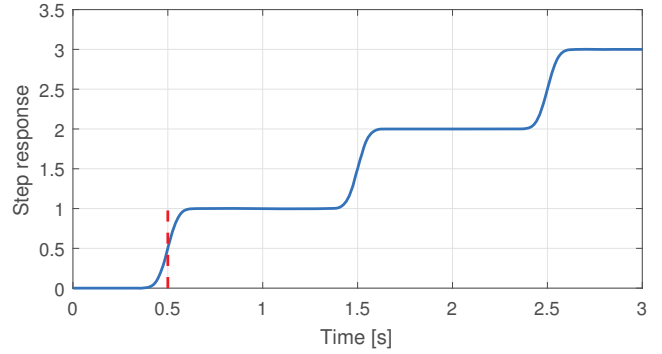


Fig. 7. The step response of (23).

Whereas a controller based on the universal signal generator (16), assuming $\gamma = 0$ and taking into account (18) and (19), can be rewritten in the form of

$$(22) \quad C_2(s) = k_{RC} G_5(s) \stackrel{\gamma=0}{=} \frac{k_{RC} \frac{1}{T} e^{-\frac{sT}{2}}}{s \prod_{n=1}^{\infty} \left(\left(\frac{sT}{2\pi n}\right)^2 + 1\right)}.$$

A similar analysis has been proposed in [18]. The authors additionally assumed that the multiresonant controller $C_1(s)$ is tuned specifically to mimic the ILC controller $C_2(s)$. This seems to be impractical, because the computational burden imposed by the multioscillatory controller is significantly higher than the one imposed by the ILC algorithm. These controllers are clearly not equivalent, because there are different degrees of freedom of the tuning procedure: k_0, k_1, \dots, k_n for the multioscillatory controller and just a single gain k_{RC} for the alternative iterative learning controller. Nevertheless, both of them introduce exactly the same generating polynomials in the continuous time domain. Thus, both of them fall into the same category of solutions derived (whether deliberately or unintentionally) within the same frame of IMP.

The ILC controller based on the universal signal generator from Fig. 6 introduces an innate delay of one reference and/or disturbance signal period. This delay might seem to be halved in (22), but obviously they have to be equivalent as (22) is equivalent to (16) for $\gamma = 0$. Note that the 'missing' half-cycle delay is introduced by the infinite product in (22). The step response of

$$(23) \quad G_6(s) = \frac{1}{s \prod_{n=1}^{25} \left(\left(\frac{s}{2\pi n}\right)^2 + 1\right)}$$

is shown in Fig. 7.

As demonstrated, in their basic form both controllers (the multiresonant one and the ILC) introduce exactly the same generating polynomials and therefore suffer from exactly the same unlimited control signal growth if the selected harmonics cannot be suppressed to zero in the control error. To make both controllers more robust, damping is necessary. A simple forgetting as in (16) is similar to keeping constant damping for all frequencies. This is illustrated in Fig. 8 and Fig. 9. Forgetting in the ILC does not have to be equal for all frequencies. It is common practice to design a problem-specific digital filter $Q(z)$ to introduce a frequency-dependent forgetting. The resulting control law is

$$(24) \quad x(k, p) = Q(z)x(k - 1, p) + k_{RC}e(k - 1, p).$$

Similar behaviour can be achieved in the multioscillatory controller by selecting a different ζ and different gains k_n for each oscillator. This is illustrated in Fig. 10, Fig. 11 and Fig. 12. This means that the flexibility of the multioscillatory controller

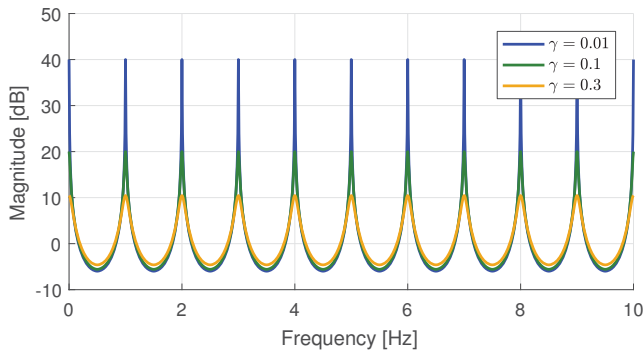


Fig. 8. Frequency characteristics for different values of γ in the ILC.

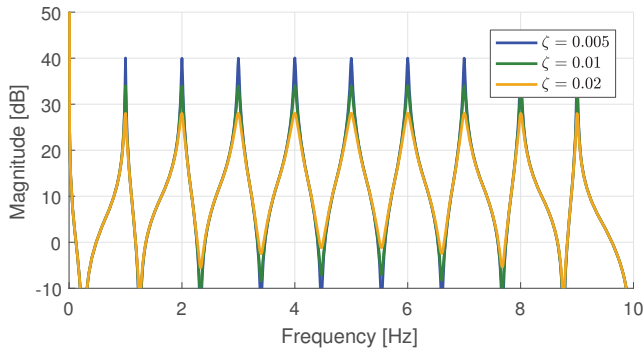


Fig. 9. Frequency characteristics for different values of ζ in the multioscillatory controller.

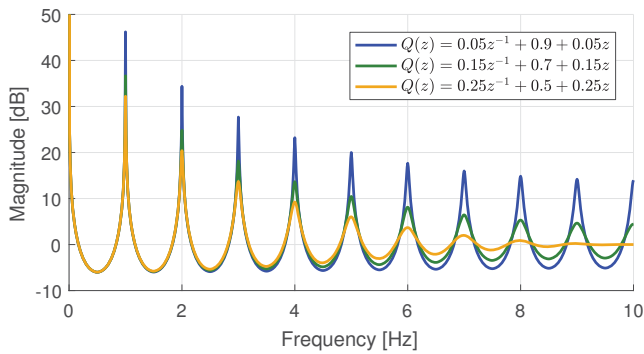


Fig. 10. Frequency characteristics for different filters $Q(z)$ in the ILC.

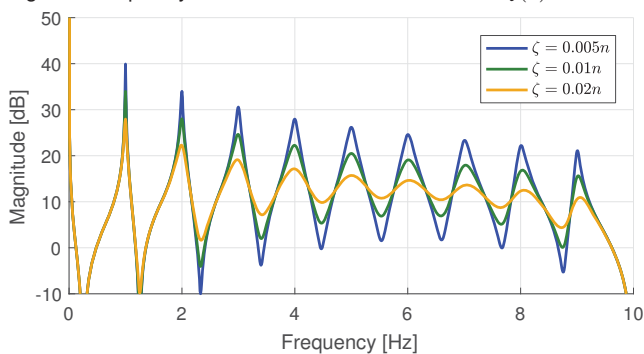


Fig. 11. Frequency characteristics for different variable ζ in the multioscillatory controller (here ζ is assumed to be proportional to the resonant frequency).

coming from the possibility of selecting individual gains and damping ratios for each oscillatory term is also present in the ILC in the form of the $Q(z)$ filter, which can be freely designed to get a desired frequency response. Our observation is that designing individual gains and damping ratios in the multioscillatory controller is usually equally cumbersome as designing the characteristics of the $Q(z)$ filter. In our opinion none of the approaches can be called a definite winner in

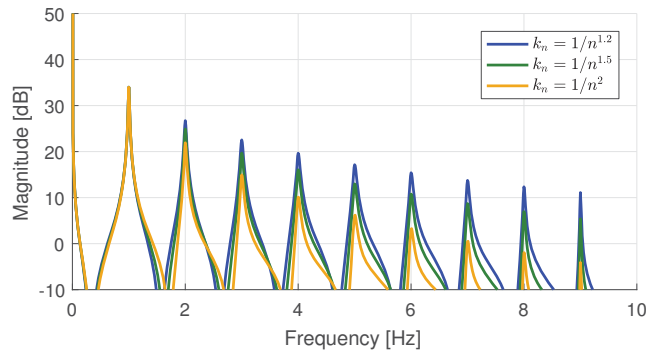


Fig. 12. Frequency characteristics for different variable k_n in the multioscillatory controller (off-the-cuff functions indicated in the legend box).

Table 1. Selected parameters of the grid-tie converter

| Parameter | Value |
|-------------------|--------------|
| Nominal power | 250 kVA |
| DC link voltage | 500 V |
| Filter inductance | 120 μ H |
| Filter resistance | 4 m Ω |

this regard. However, there is one clear distinction between these two approaches – the delay. The ILC controller (22) has the intrinsic delay of one period of the fundamental frequency, and this delay cannot be shaped during the design procedure. On the other hand, the multioscillatory controller (20) introduces zeros and the control signal is modified instantaneously, i.e. after one sample period. In this respect, we tend to believe that the multioscillatory controller may be more beneficial in selected applications.

Periodic disturbance rejection in a grid-tie converter

Both controllers have been tested in a grid-tie converter shown in Fig. 13 of key parameters collated in Tab. 1.

The test scenario assumes introducing significant distortion in the grid voltage – the ideal sinusoidal grid voltage is instantaneously changed into a trapezoidal one, of a harmonic content shown in Fig. 14, and then relaxed back to the sinusoidal one. The control algorithm includes a phase lock loop (PLL) to track the phase of the fundamental component of the distorted three-phase grid voltage. The original ‘PLL (3ph)’ block available in MATLAB has been used without any modifications. The shape of the grid current under distorted conditions if no repetitive control is switched on, i.e. only the PI controllers are on and the DFF is deactivated, is shown in Fig. 15. Steady-state grid currents for multioscillatory controllers (6th, 12th, 18th harmonics and $\zeta = 0.01$) are juxtaposed in Fig. 16 with the grid currents shaped by the iterative learning controller ($\gamma = 0.01$). The corresponding transient states are shown in Fig. 17. The evolution of the MSE (mean square error calculated over the entire period of the reference current) is shown in Fig. 18. Regarding the selection of the resonant frequencies for this experiment, it should be mentioned that e.g. the 5th harmonic (negative sequence) and the 7th harmonic (positive sequence) both transform into the 6th harmonic in the rotating reference frame aligned with the fundamental harmonic.

In this particular comparison, it might seem that the multioscillatory controller (MOSC) is superior. However, it has to be noted that both controllers are tuned by guessing and checking here. Therefore, this might rather suggest that the MOSC is easier to handle by guessing and checking and indeed this is our impression. It was also observed that assuming the goal of comparative steady states for both con-

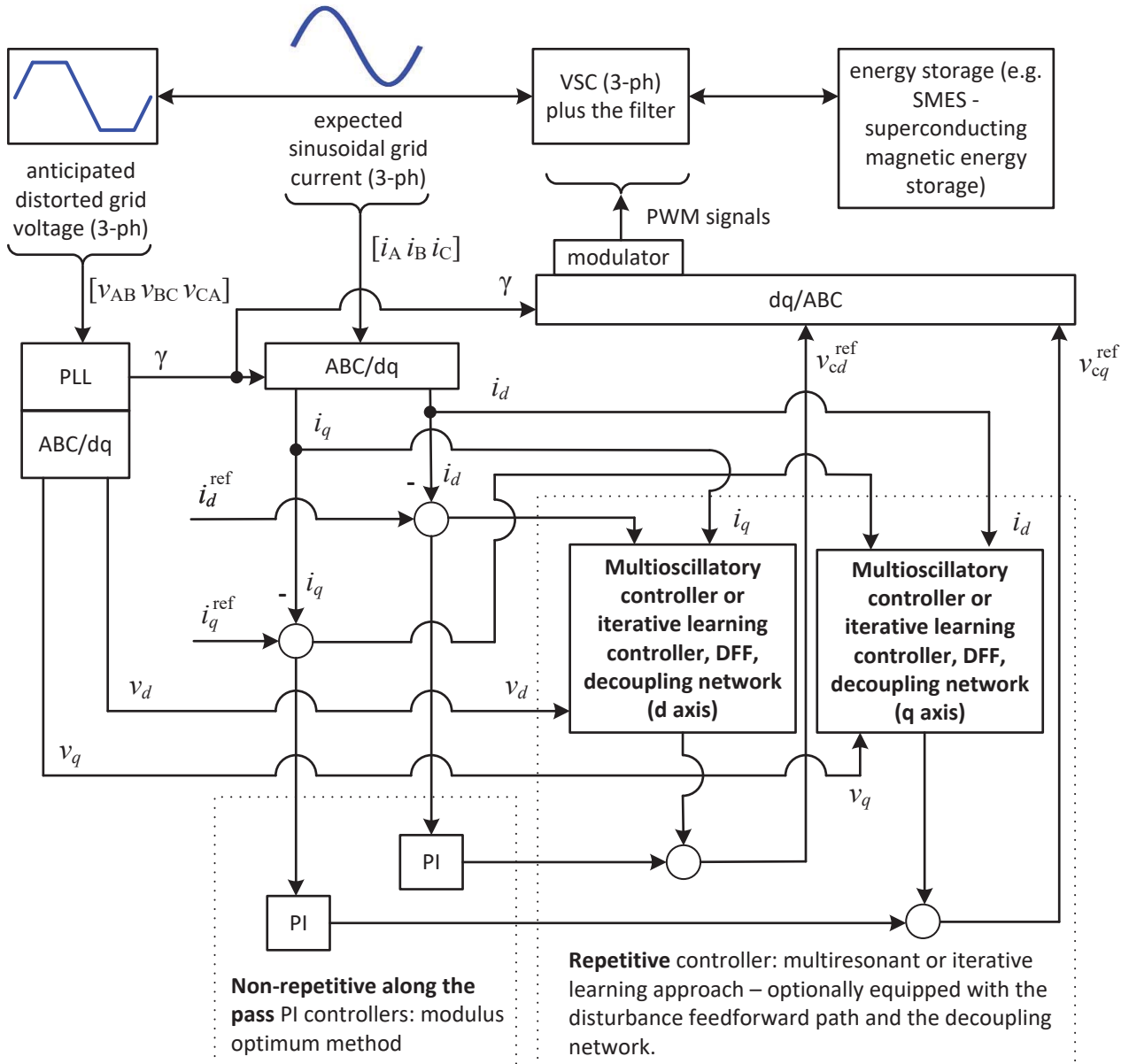


Fig. 13. The topology of the current control system.

trollers, we tended to run into numerical problems earlier in the case of the MOSC. This is related to the problematic oscillatory element implementation near the Nyquist frequency. The control signal may be corrected faster in an MOSC based system, yet this comes at the expense of greater sensitivity of the performance to the controller discretization process.

Let us summarize our observations in Tab. 2. The proposed ratings should be regarded as some kind of soft guidelines. One should not interpret them as definite ones.

Periodic disturbance feedforward in the context of repetitive control

There is a notion among repetitive control practitioners, especially prevalent among ILC engineers, that a successful control law should focus on IMP. This is true, but only partially. It should be noted that a more logical design flow is one that starts from a feedforward controller(s), which is (are) then augmented using a feedback controller. The feedback controller is there only to compensate for all the uncertainties.

In the case of the grid-tie converter, theoretically it is possible to design an ideal disturbance feedforward (DFF) path, and its synthesis requires the knowledge of only one state

variable, namely the DC link voltage, and the grid voltage, as in

$$(25) \quad v_d = Ri_d + L \frac{di_d}{dt} - \omega_1 Li_q + v_{cd}$$

$$(26) \quad v_q = Ri_q + L \frac{di_q}{dt} + \omega_1 Li_d + v_{cq},$$

where: $[v_d, v_q]$ is the grid voltage, $[v_{cd}, v_{cq}]$ is the converter voltage and ω_1 denotes the angular speed of the reference frame equal to the fundamental grid angular frequency. Both of them are already measured in the system: the grid voltages to facilitate a PLL, which is needed to orient the reference frame, and the DC link voltage to implement a DC-link voltage control loop. To get sinusoidal grid currents it is enough to add the measured grid voltage (i.e. the disturbance), scaled using a DC-link voltage value, to the converter control signal, as in

$$(27) \quad v_{cd}^{ref} = \underbrace{v_d}_{DFF} - \underbrace{\left(Ri_d + L \frac{di_d}{dt} \right)}_{PI} + \underbrace{\omega_1 Li_q}_{\text{decoupling network}}$$

Table 2. Comparison of ILC and MOSC

| Controller Feature | ILC with γ | ILC with $Q(z)$ | MOSC (a few of terms) | MOSC (many of terms) |
|----------------------------------|---------------------------------|---------------------------------|-----------------------|------------------------|
| computational burden | low | medium | high | very high |
| memory burden | medium | medium | low | low |
| analytical tuning | cumbersome | non-existent | challenging | very challenging |
| expert tuning | easy | challenging | practical | challenging |
| responsiveness | low | low | high | high |
| speed vs. robustness | poor | poor | good | good |
| robustness to grid freq. fluct. | very poor* | very poor* | good [†] | good [†] |
| sensitivity to delays | easy to compensate [‡] | easy to compensate [‡] | poor [§] | very poor [§] |
| recognition in robotics | high | high | low | low |
| recognition in power electronics | low | low | high | high |

* unless an additional adaptive fractional delay filter is implemented, which has already been demonstrated in the case of grid converters [2, 19, 20, 21, 22];

[†] very good if the oscillatory terms are of an adaptive type, which is fairly easy to achieve because the grid frequency is already available thanks to the PLL;

[‡] by modifying (24) into $x(k, p) = Q(z)x(k-1, p) + k_{RC}e(k-1, p + p_0)$ and setting a proper value of p_0 [2, 19];

[§] unless oscillatory terms are individually modified to obtain the phase lead [23, 16, 24] (with corrections in [25]).

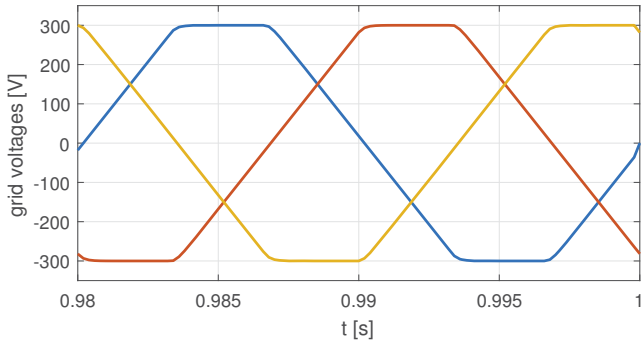


Fig. 14. A distorted grid voltage and its harmonic content (scaling: relative, linear).

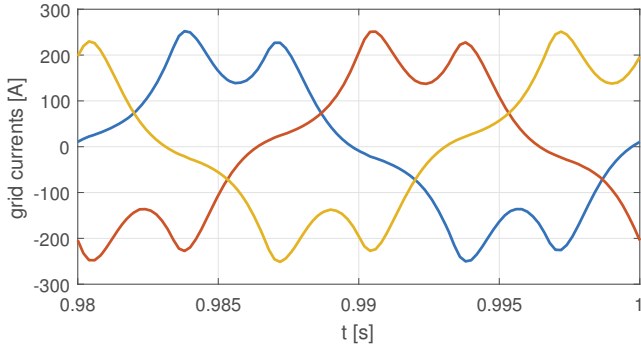


Fig. 15. Grid current under non-repetitive control.

$$(28) \quad v_{cq}^{\text{ref}} = \underbrace{v_q}_{\text{DFF}} - \underbrace{\left(Ri_q + L \frac{di_q}{dt} \right)}_{\text{PI}} \underbrace{-\omega_1 Li_d}_{\text{decoupling network}}.$$

This DFF is already present in most practical solutions of grid

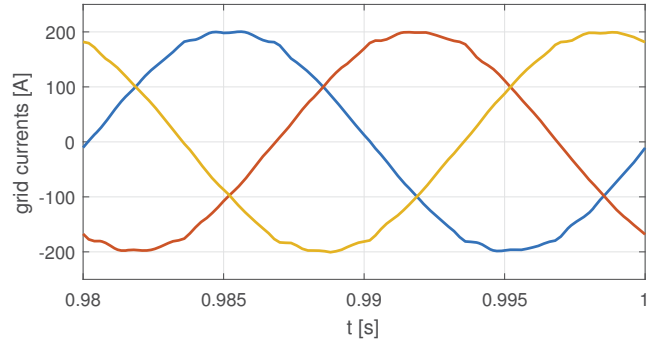
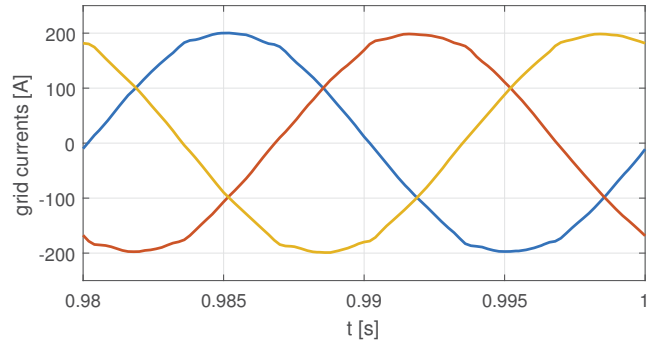


Fig. 16. A steady-state grid current under ILC (with $Q(z) = 0.25z + 0.5 + 0.25z^{-1}$) and MOSC (with 6^{th} , 12^{th} and 18^{th} harmonics cancellation) comparison.

converters – it is needed to synchronise converter voltage with the grid voltage before switching on the current controllers to avoid an initial current surge. If no DFF is implemented, the measured grid voltage represented in the dq reference frame has to be used to determine the initial conditions for integrators in the PI controllers shown in Fig. 13. The theoretical full DFF for this converter is of a static form, i.e. it does not require any dynamical internal model to be implemented to fully reject the disturbance (here the distorted grid voltage) and totally eliminate any transient states related to this disturbance. This is illustrated in Fig. 19.

Unfortunately, any practical digital implementation of this DFF is bound to introduce a delay of at least one sample time period and this renders the disturbance rejection partial only (see Fig. 19). That is why it is necessary to support the DFF

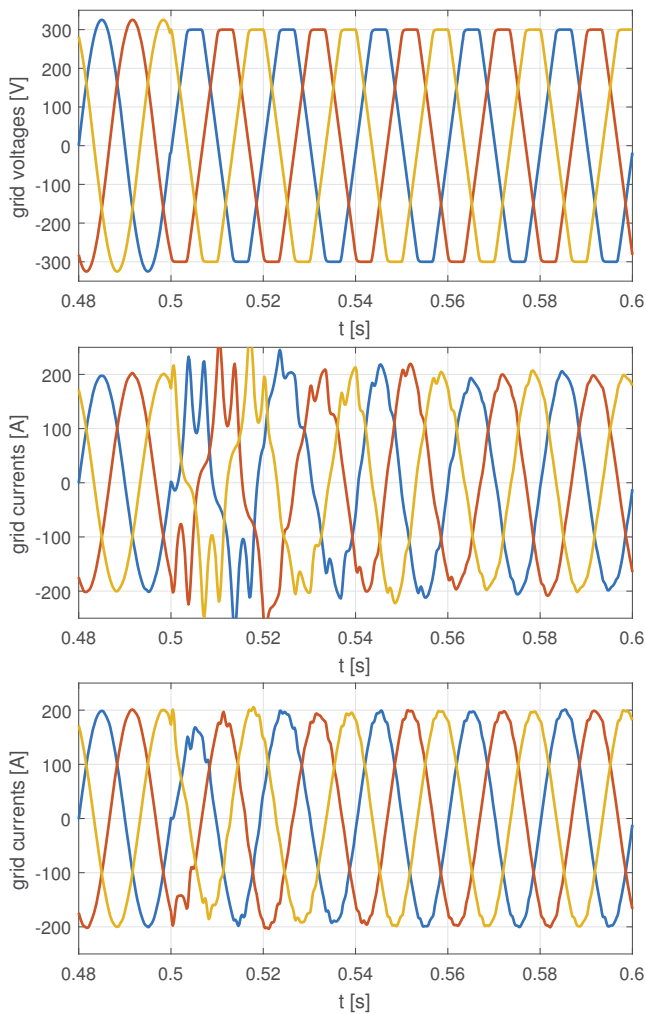


Fig. 17. A transient grid current under ILC and MOSC comparison.

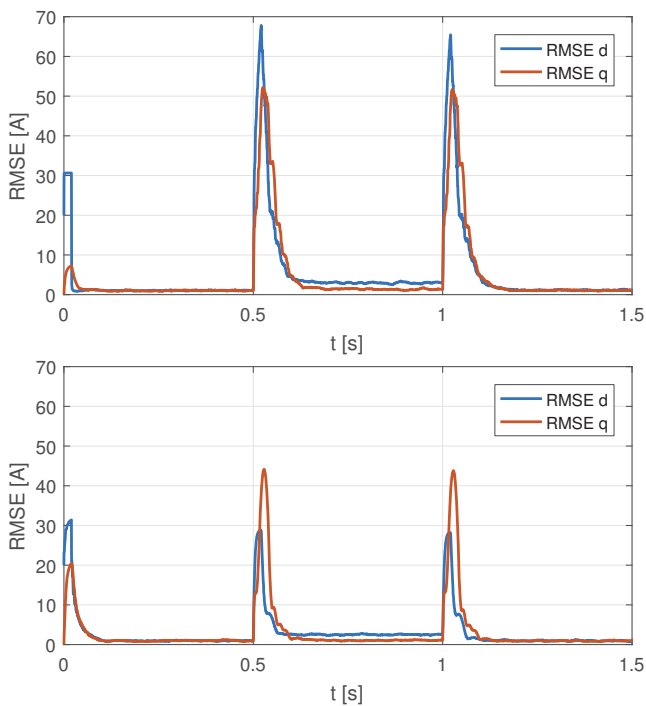


Fig. 18. RMSE evolution under ILC and MOSC comparison showing the typically slower responsiveness of the ILC system.

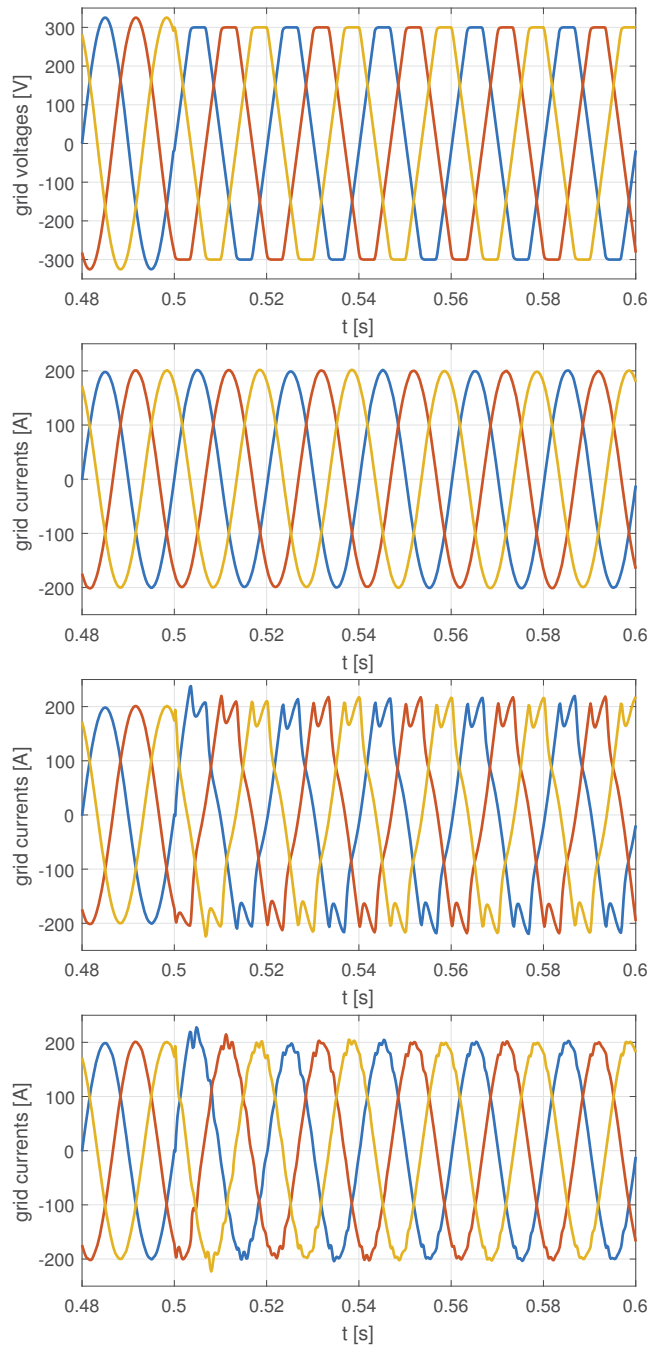


Fig. 19. A transient grid current under DFF, delayed DFF and delayed DFF with MOSC comparison (also to be compared with no DFF scenario in Fig. 17).

with e.g. an MOSC in order to achieve an undistorted current in the steady state (see Fig. 19), i.e. to have

$$(29) \quad v_{cd}^{\text{ref}} = \underbrace{v_d^{\text{delayed}}}_{\text{partial DFF}} - \underbrace{(v'_d + Ri_d + L \frac{di_d}{dt})}_{\text{PI+MOSC}} + \underbrace{\omega_1 Li_q}_{\text{decoupling network}}$$

$$(30) \quad v_{cq}^{\text{ref}} = \underbrace{v_q^{\text{delayed}}}_{\text{partial DFF}} - \underbrace{(v'_q + Ri_q + L \frac{di_q}{dt})}_{\text{PI+MOSC}} - \underbrace{\omega_1 Li_d}_{\text{decoupling network}},$$

where

$$(31) \quad v'_d = v_d^{\text{delayed}} - v_d$$

$$(32) \quad v'_q = v_q^{\text{delayed}} - v_q$$

represent the uncertainties (here measurement errors, inter alia, due to the delay of the digital control system). The DFF considerably improves transient states – the MOSC is here only to compensate for the innate delay of the digital control system related to sampling and potential signal conditioning (e.g. anti-aliasing filters).

Conclusions

The iterative learning control and the multioscillatory (a.k.a. multiresonant) controllers are both based on the same principle of internal model, and both in their basic form introduce exactly the same generating polynomials to the controller. This is not an original nor a ground-breaking conclusion, yet often an under-recognized one. Both approaches have their strengths and weaknesses and none of them should be regarded as the definitive winner for power electronics control engineers. Moreover, more of these weaknesses are common for both types of the discussed repetitive controllers and selecting one of them is often predicated on the familiarity with one type and the lack of such familiarity with the other type. This paper is aimed at making this choice more fact-based and reducing the familiarity-induced bias. To save the paper from being overstuffed, only key plots are included. Many other ILC, MOSC and DFF test scenarios can be generated using the numerical models published on MATLAB Central [26].

The research was partially supported by the National Centre for Research and Development (Narodowe Centrum Badań i Rozwoju) within the project No. PBS3/A4/13/2015 entitled "Superconducting magnetic energy storage with a power electronic interface for the electric power systems" (original title: "Nadprzewodzący magazyn energii z interfejsem energoelektronicznym do zastosowań w sieciach dystrybucyjnych"), 01.07.2015–31.12.2018. The acronym for the project is NpME.

Authors: Bartłomiej Ufnalski, PhD, DSc, prof. Lech M. Grzesiak, PhD, DSc, Arkadiusz Kaszewski, PhD, MSc, Andrzej Galecki, MSc, Institute of Control and Industrial Electronics, Faculty of Electrical Engineering, Warsaw University of Technology, 75 Koszykowa St., Warsaw 00-662, Poland, email: bartlomiej.ufnalski@ee.pw.edu.pl

REFERENCES

- [1] Xu M. X., Xu D., Lin P., Chen M., Ni J., Zhang T.: Understanding repetitive control and resonant control, 3rd IEEE International Symposium on Power Electronics for Distributed Generation Systems (PEDG), pp. 621–627, Aalborg, 2012.
- [2] Nazir R.: Advanced repetitive control of grid converters for power quality improvement under variable frequency conditions, Ph.D. Dissertation, University of Canterbury, Christchurch, New Zealand, 2015.
- [3] Francis B. A., Wonham W. M.: The internal model principle of control theory, *Automatica*, vol. 12, pp. 457–465, Pergamon Press, 1976.
- [4] Bengtsson G.: Output regulation and internal models – a frequency domain approach, *Automatica*, vol. 13, pp. 333–345, Pergamon Press, 1977.
- [5] Ludwick S. J., Profeta J. A.: A user's guide to repetitive control systems and the internal model principle, http://www.aspe.net/publications/Spring_2010/Spr10Ab/3006Ludwick.pdf, Aerotech, Inc., Pittsburgh, PA, USA
- [6] Żak S. H.: The internal model principle, https://engineering.purdue.edu/~zak/ECE_382-2014/hand_3.pdf, ECE 382 Fall 2016 course handouts, Purdue University, 2016.
- [7] Li P.: Internal model principle, <http://www.me.umn.edu/courses/me8281/Old/IMP-repetitive.pdf>, ME 8281 Spring 2006 course handouts, University of Minnesota, 2006.
- [8] Wang Y., Gao F., Doyle F. J.: Survey on iterative learning control, repetitive control, and run-to-run control, *Journal of Process Control*, vol. 19, pp. 1589–1600, 2009.
- [9] Dabkowski P., Galkowski K., Rogers E., Sebek M.: Robustness of uncertain discrete linear repetitive processes with disturbance attenuation, *European Control Conference (ECC)*, Aalborg, pp. 2288–2293, 2016.
- [10] Ufnalski B., Grzesiak L.: Repetitive neurocontroller with disturbance feedforward path active in the pass-to-pass direction for a VSI inverter with an output LC filter, *Bulletin of the Polish Academy of Sciences – Technical Sciences, PAN*, vol. 64, no. 1, pp. 115–125, 2016.
- [11] Ufnalski B., Grzesiak L.: Plug-in direct particle swarm repetitive controller with a reduced dimensionality of a fitness landscape – a multi-swarm approach, *Bulletin of the Polish Academy of Sciences – Technical Sciences, PAN*, vol. 63, no. 4, pp. 857–866, 2015.
- [12] Ufnalski B., Grzesiak L. M., Malkowski M.: Hybridization schemes for particle swarm iterative learning controllers in repetitive systems, *European Power Electronics (EPE'17 ECCE Europe) Conference*, Warsaw, 2017.
- [13] Ufnalski B.: Hybrid swarm-based repetitive controller with adaptive forgetting for a grid-tie converter, <https://www.mathworks.com/matlabcentral/fileexchange/64056-hybrid-swarm-based-repetitive-controller-with-adaptive-forgetting-for-a-grid-tie-converter>, August 2017.
- [14] Galecki A., Michalczyk M., Kaszewski A., Ufnalski B., Grzesiak L.: Multi-oscillatory current control with anti-windup for grid-connected VSCs operated under distorted grid voltage conditions, *European Power Electronics (EPE'17 ECCE Europe) Conference*, Warsaw, 2017.
- [15] Wikipedia: Bilinear transform, https://en.wikipedia.org/wiki/Bilinear_transform, accessed on 18.07.2017.
- [16] Yepes A. G.: Digital resonant current controllers for voltage source converters, <http://agyepes.webs.uvigo.es/files/Thesis.pdf>, PhD dissertation, University of Vigo, Spain, 2011.
- [17] Wolfram Research: <http://functions.wolfram.com/ElementaryFunctions/Sinh/>, accessed on 21.07.2017.
- [18] Xu M. X., Xu D., Lin P., Chen M., Ni J., Zhang T.: Understanding repetitive control and resonant control, 3rd IEEE International Symposium on Power Electronics for Distributed Generation Systems (PEDG), pp. 621–627, Aalborg, 2012.
- [19] Nazir R.: Taylor series expansion based repetitive controllers for power converters, subject to fractional delays, *Control Engineering Practice*, vol. 64, pp. 140–147, 2017.
- [20] Nazir R., Wood A., Laird H., Watson N.: An adaptive repetitive controller for three-phase PWM regenerative rectifiers, *International Conference on Renewable Energy Research and Applications (ICRERA)*, Palermo, pp. 1126–1131, 2015.
- [21] Yang Y., Zhou K., Blaabjerg F.: Enhancing the frequency adaptability of periodic current controllers with a fixed sampling rate for grid-connected power converters, *IEEE Transactions on Power Electronics*, vol. 31, no. 10, pp. 7273–7285, 2016.
- [22] Yang Y., Zhou K., Blaabjerg F.: Frequency adaptability of harmonics controllers for grid-interfaced converters, *International Journal of Control*, 90:1, 3–14, 2017.
- [23] Wang X., Blaabjerg F., Loh P. C.: Design-oriented analysis of resonance damping and harmonic compensation for LCL-filtered voltage source converters, *International Power Electronics Conference (IPEC – ECCE ASIA)*, pp. 216–223, 2014.
- [24] Yepes A. G., Freijedo F. D., Lopez O., Doval-Gandoy J.: High-performance digital resonant controllers implemented with two integrators, *IEEE Transactions on Power Electronics*, vol. 26, no. 2, pp. 563–576, 2011.
- [25] Yepes A. G., Freijedo F. D., Lopez O., Doval-Gandoy J.: Correction to "High performance digital resonant controllers implemented with two integrators", *IEEE Transactions on Power Electronics*, vol. 27, no. 10, pp. 4357–4357, 2012.
- [26] Ufnalski B.: ILC vs. MOSC, <https://www.mathworks.com/matlabcentral/fileexchange/64036-ilc-vs-mosc>, November 2017.